Structural characterization of semicrystalline polymer morphologies by imaging-SANS

2012 J. Phys.: Conf. Ser. 340 012089

(http://iopscience.iop.org/1742-6596/340/1/012089)

Structural characterization of semicrystalline polymer morphologies by imaging-SANS

A Radulescu[1], L J Fetters[2] and D Richter[3]

[1]Forschungszentrum Jülich GmbH, Jülich Centre for Neutron Science, Outstation FRMII, 85747 Garching, Germany

[2]School of Chemical and Biomolecular Engineering, Cornell University, Ithaca, NY 14853-5021, USA

[3]Forschungszentrum Jülich GmbH, Jülich Centre for Neutron Science and Institute for Complex Systems, 52425 Jülich, Germany

a.radulescu@fz-juelich.de

Abstract. Control and optimization of polymer properties require the global knowledge of the constitutive microstructures of polymer morphologies in various conditions. The microstructural features can be typically explored over a wide length scale by combining pinhole-, focusing- and ultra-small-angle neutron scattering (SANS) techniques. Though it proved to be a successful approach, this involves major efforts related to the use of various scattering instruments and large amount of samples and the need to ensure the same crystallization kinetics for the samples investigated at various facilities, in different sample cell geometries and at different time intervals. With the installation and commissioning of the MgF_2 neutron lenses at the KWS-2 SANS diffractometer installed at the Heinz Maier-Leibnitz neutron source (FRMII reactor) in Garching, a wide *Q*-range, between 10^{-4}Å^{-1} and 0.5Å^{-1}, can be covered at a single instrument. This enables investigation of polymer microstructures over a length scale from 1nm up to 1μm, while the overall polymer morphology can be further examined up to 100μm by optical microscopy (including crossed polarizers). The study of different semi-crystalline polypropylene-based polymers in solution is discussed and the new imaging-SANS approach allowing for an unambiguous and complete structural characterization of polymer morphologies is presented.

1. Introduction

The macroscopic behavior of semicrystalline polymers depends on the constitutive microstructures consisting of molecules arranged in the unit cell (~Å), lamellar crystals (~100Å), fibrils or boards (~1000Å) and spherulitic macro-aggregats (>1μm). Control and optimization of polymer properties require the global knowledge of these microstructural features in various conditions. Such a wide length scale can be explored by combining conventional pinhole-, focusing- and ultra-SANS techniques [1] which enable to cover a *Q*-range typically between 10^{-5}Å^{-1} and 0.2-0.3Å^{-1}. This approach, which permits the exploration of independent or interrelated structural levels emerging within a length scale from 10Å up to 10μm, was often applied for the quantitative characterization of the morphology of a wide range of materials, from hydrogels to geologic samples [2]. Optical and

transmission electron microscopy observations have often been used complementary to the ultra-SANS investigations, in order to help for the assessment of the scattering data.

This combination of scattering methods proved to be successful in resolving the structure and morphology of complex systems showing a hierarchical multi-scale organization [3-8]. The investigation of crystallization behavior of polymers from melt or solution requires in this case a special attention. Occurrence and evolution of microstructures in a semicrystalline polymer depend strongly on the crystallization conditions which are defined and controlled by the experimental items, like the variation and control of temperature and the amount and geometry of sample. Thus, major efforts that must ensure the same crystallization kinetics for the sample studied at various experimental facilities (diffractometers, neutron sources, etc.), in different sample cell geometries and at different time intervals are involved. The access of a wide *Q*-range at the same diffractometer solves such problems and allows for a complete and unambiguous characterization of the structures and morphologies arising from crystallization processes in an easier way.

In this paper we report about the exploration of the multilevel structures that form upon cooling in solution of polypropylene-based semicrystalline polymers by using two imaging-SANS approaches based on the combination of small-angle neutron scattering and microscopy methods. The first approach implies the combination of three SANS techniques: conventional SANS at the KWS-2 classical pinhole SANS diffractometer [9,10], focusing-mirror SANS (f-SANS) at the KWS-3 very-SANS instrument [11,12] and ultra-SANS at the double-crystal diffractometer DKD [13]. The configuration of the instruments at the FRJ-2 reactor in Jülich will be briefly presented and the experimental results discussed. Optical microscopy with crossed polarizers was used complementary to the ultra- and f-SANS investigations. The second experimental approach it is since recently in use at the KWS-2 diffractometer, which was re-installed in 2007 at the FRMII reactor in Garching. This approach implies for the observation of a wide-*Q* range, between 10^{-4}Å^{-1} and 0.5Å^{-1}, the use of neutron lenses (MgF_2 optical elements [14-16]) besides the classical pinhole set-up. The use of optical microscopy for the investigation of the large-scale morphologies several micrometers in size it is a prerequisite condition for the complete characterization of the complex aggregates in this case.

2. Experimental section

2.1. Samples

A syndiotactic polypropylene homopolymer *s*PP and a multiblock atactic-isotactic alternating polypropylene (*a*PP-*i*PP) copolymer were studied by SANS, f-SANS and ultra-SANS in dilute solutions (polymer volume fraction Φ_{pol}=0.5%) in deuterated decane (d-22) or dodecane (d-26). The polymers were prepared via a living polymerization in toluene at 0°C using a bis(salicylaldiminato)titanium complex. Details about the synthesis of polymers are presented elsewhere [3,17]. The self-assembling structural features of two materials, a *s*PP polymer with the molecular weight M_W=61.4kg/mol (M_W/M_n=1.1) and a *a*PP-*i*PP alternating copolymer with the M_W=107kg/mol (M_W/M_n=2), were investigated at room temperature.

For testing the performance of the focusing lenses at the KWS-2 SANS instrument a poly(methymethacrylate) (PMMA) colloidal sample (R=7760Å) was investigated. The obtained results have been compared with those obtained at the focusing-mirror KWS-3 instrument on a similar sample [18]. In order to minimize the effects arising from multiple scattering, h-PMMA dissolved in h-cis-decalin (0.25% colloids volume fraction) was measured, which provided a reasonable contrast condition and an acceptable sample transmission [18].

Finally, a crystalline-amorphous *s*PP-P(E-*co*-P) diblock copolymer was investigated in a deuterated decane (d-22) solution (Φ_{pol}=1%) at KWS-2 diffractometer using the combined conventional pinhole and focusing-lenses modes.

2.2. SANS techniques

Three types of SANS techniques were used at the FRJ-2 reactor. The conventional SANS measurements were performed on the KWS-2 pinhole instrument using a neutron wavelength of λ=7.2Å ($\Delta\lambda/\lambda$=10%) and a sample-to-detector distance varying from 2 to 20m, covering a *Q* range between 0.002 and 0.14Å^{-1}, where Q is the modulus of the scattering vector, $4\pi(\sin\theta)/\lambda$, with θ being half the scattering angle. The raw data were corrected two dimensionally for the empty cell scattering and detector sensitivity and were calibrated in absolute units using a Plexiglas secondary standard [9]. The KWS-3 focusing-mirror SANS instrument [11,12] works on a principle based on a one-to-one image of an entrance aperture on a two-dimensional high-resolution position-sensitive detector (0.5mm spatial resolution)by neutron reflection from a double focusing toroidal mirror. A small entrance aperture (typically 2x2mm^2) and the neutron wavelength λ=12.7Å ($\Delta\lambda/\lambda$=9%) permitted SANS studies within a *Q* range 1x10^{-4} to 2x10^{-3}Å^{-1}. The ultra-SANS measurements were performed at the DKD double-crystal diffractometer, which, operating with a neutron wavelength λ=4.5Å, could cover a *Q* range between 3x10^{-5} and 2x10^{-4}Å^{-1}. The high-*Q* resolution existed in one dimension only, therefore, in order to present the measured data in continuation to those measured at KWS-2 and KWS-3, slit corrections had to be applied [13].

At KWS-3 and DKD instruments the multiple scattering effects were very important and dominated for sample thicknesses within the range 1-2mm, typical for conventional pinhole-SANS experiments [11]. To minimize the contribution of such effects and to have a reasonable sample transmission (higher than 70%) one had either to decrease the path length, dilute the sample (to nearly infinite dilution), or one had to decrease the contrast by using a certain fraction of protonated solvent.

Following the shutdown of the FRJ-2 reactor the KWS-2 and KWS-3 instruments have been moved to the Heinz Maier-Leibnitz neutron source (FRMII reactor) in Garching. Here, the much higher flux allows at KWS-2 for the use of longer wavelengths, up to 20Å, thus enabling much lower values in *Q*, up to 7x10^{-4}Å^{-1}, in the pinhole configuration. A further decrease in *Q* up to 10^{-4}Å^{-1} is possible by means of focusing elements – the MgF_2 lenses [14-16], which are used in the combination with a small entrance aperture, at the longest collimation length of 20m. The conceptual design and the preliminary tests using aspherical lenses are reported in detail elsewhere [15]. Here, we present some additional results of testing the performance of lenses and report about the complete characterization of the *s*PP-P(E-*co*-P) structures in solution by combining the pinhole and the focusing-lenses modes. This proved to be a suitable experimental approach for the exploration of structural features over a wide length scale on samples like semicrystalline polymers requiring a special care with respect to variation of the environmental conditions. In the present study seven lenses have been used with a high-resolution detector (space resolution of 0.5mm) placed at 8.9m distance from the lenses and a small collimation aperture (6x6mm^2) placed at 18.2m in front of the lenses. The neutron wavelength used was λ=17.6Å and the sample size (sample aperture) was 1.5cm x 2.5cm. A beam-stop of 4x4mm^2 was used in order to mask the direct beam focused on the detector.

Finally, optical microscopy using a Zeiss-Axioplan-2 microscope in transmission bright field direct geometry equipped with a Linkam THMS600 temperature stage was involved in the study. Polarized light with crossed polarizers was used to complete the characterization of some of the morphologies identified. The technique was always used as a complementary method to the ultra- and f-SANS investigations and served for the assessment of the scattering data. For the case of exploring a wide Q range only at the KWS-2 instrument, the optical microscopy becomes necessarily used for the determination of the morphology and size of the large scale macro-aggregates within the micrometer range.

3. Modelling and Data Interpretation

Self-assembly and crystallization from solution of semicrystalline polymers often result in complex morphologies displaying multiple structural levels on length scale ranging from nanometers to microns. The combination of scattering data with fractal geometry concepts recently commenced to

become a general path of investigating such systems. Fractal models describe power law regimes often observed in measured scattering profiles [19-21] with the exponents depending on the geometric structure of the scattering objects:

$$\frac{d\Sigma}{d\Omega}(Q) \approx Q^{-p} \tag{1}$$

Hence, one-dimensional (p=1), platelet-like (p=2), mass fractals ($1 \le p \le 3$), or surface fractals ($3 \le p \le 4$) structures can be identified and characterized. Objects with smooth surface yield p=4 (Porod scattering), whereas diffuse interfaces lead to the occurrence of exponents higher than p=4 [22].

The analysis of the extensive scattering data in Q has been done in terms of the Beaucage model [20,21], which describes material microstructure in terms of level of structure where each level is characterized by a Guinier regime combined with a structurally limited power law regime. With two size limits ($QR_{gi} \approx 1$ and $QR_{g(i+1)} \approx 1$) for one structural level, the model describes an arbitrary number of interrelated structural features on different size scales by:

$$\frac{d\Sigma}{d\Omega}(Q) = \sum_{i=1}^{m} G_i \exp\left(\frac{-Q^2 R_{gi}^2}{3}\right) + B_i \exp\left(\frac{-Q^2 R_{g(i+1)}^2}{3}\right)\left[\frac{\left(erf\left(QR_{gi}/\sqrt{6}\right)\right)^3}{Q}\right]^{p_i} \tag{2}$$

where m is the number of structural levels observed in the scattering pattern extending over many decades in Q. The first term describes a large structure of average size R_{gi} composed of small-scale structures of average size $R_{g(i+1)}$. The second term allows for different morphology for the large structure according to (1). G is the classical Guinier prefactor ("forward scattering"), while B is a prefactor specific tot the type of power law regime [20,21].

Alternatively, in some cases, the scattering data from aggregates were evaluated using the traditional form factor approach [23].

4. Results and Discussion

Figure 1 presents the scattering profile at room temperature from the 0.5% solution of *s*PP polymer in d-22 measured over four decades in Q by combining the SANS, f-SANS and ultra-SANS methods. The sample was cooled in a controlled way (1°C/min) from the single coil regime, at 160°C. The power law exponent specific for the characteristic structures formed by the polymer is also indicated.

The scattering profile at intermediate and high Q follows a Q^{-2} behavior, which is indicative of polymer two-dimensional or platelet-like aggregates. The intensity drop at high Q relates to the lateral profile of the polymer platelets. The lateral extension of the platelets must exceed 3500Å, which corresponds to the lowest extension in Q of the platelets scattering profile. At lower Q the scattering intensity increases dramatically following a steep power law with an exponent higher than 4 and terminates in a Guinier-like regime at very low Q. This observation shows the formation of large-scale aggregates exhibiting diffuse interfaces and sizes within the micrometer range. For a more detailed characterization of these aggregates, optical microscopy observations have been done complementary to the ultra- and f-SANS investigations.

Figure 2 presents two micrographs collected from the polymer solution at room temperature. Open spherical aggregates with sizes around 10μm made by radially disposed smaller structures can be observed. The crossed polarizers observation of these aggregates revealed a texture which is typical for spherulitic morphology. A polymer spherulite represents a spheriform cluster of primary fiber-like or elongated lamellar crystallites that start growing laterally from the nucleation site [24]. The typical pattern yielded by a spherulitic texture when is observed with crossed polarizers is the "Maltese cross", which is observed in figure 2-right.

The scattering and microscopy data are completing each other. The scattering profile collected over a wide Q-range revealed formation of lamellar structures and large aggregates with diffuse interfaces several micrometers in size. The microscopy observations proved that these structures are interrelated and represent different structural levels of a hierarchical morphology: the polymer spherulite represents the large scale structural level which is composed of small-scale elongated lamellar

substructures that basically exhibit two structural levels, their lateral extension and width. Due the crossover between the high-Q scattering feature of spherulites and the low-*Q* scattering feature of the lamellae, in the scattering pattern collected over an extended Q range only two of these structural levels can be observed, namely the size of the spherulites and the thickness of the lamellae.

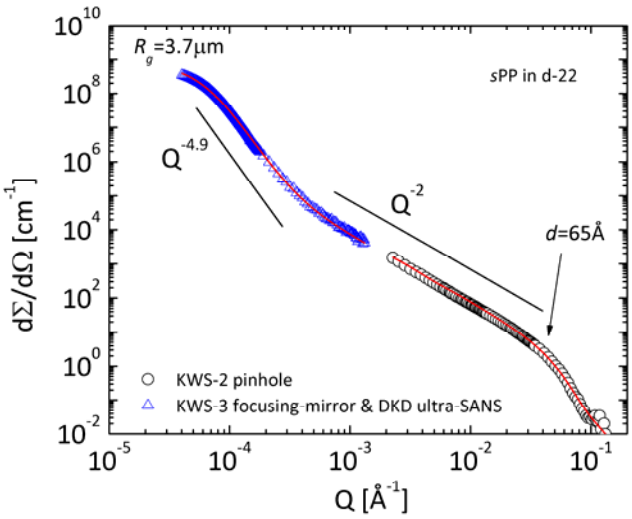

Figure 1. Wide-*Q* scattering pattern from solution of *s*PP homopolymer in d-22 at room temperature. The straight lines represent the power law behavior in different *Q* regions, whereas the solid red curve represents the model description of experimental data according to the multi-level Beaucage model (2). The main structural parameters delivered by the model analysis are also indicated.

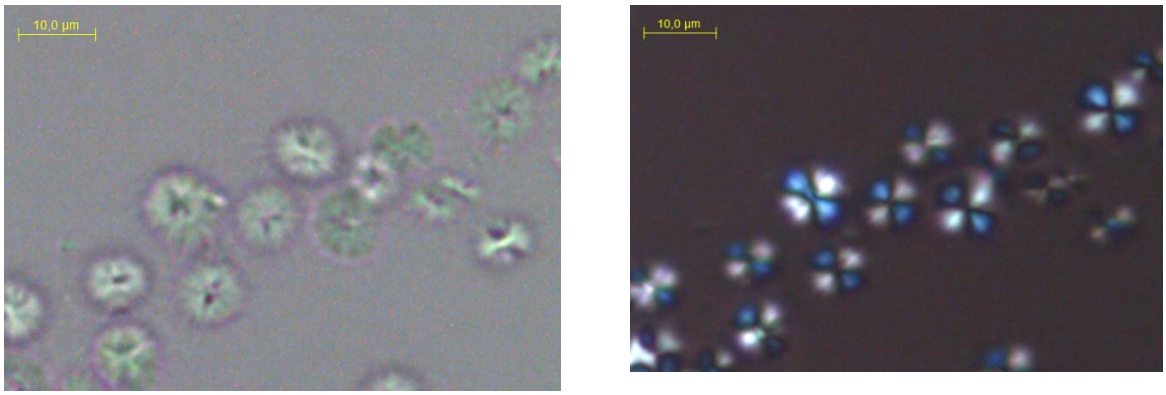

Figure 2. Morphologies of *s*PP homopolymer in d-22 observed under microscope using the bright field (left) and crossed polarizers (right); the scale bars represent 10µm.

A fit of the scattering data using the multilevel equation of Beaucage (2), which is also shown in figure 1, delivered the sizes (R_g of the spherulites and thickness *d* of the lamellae) and density parameters of the two structures. Using the obtained forward scattering and the lamellar thickness *d* and supposing compact lamellae, the total volume fraction of polymer inside the platelets coincides with the polymer volume fraction in the initial solution, which shows that all polymers are crystallizing at room temperature. With this information, using the "forward scattering" from the

spherulites and their size, the volume fraction which is occupied by the polymer inside the spherulite is about 30%, which shows the open aspect of these macro-aggregates. It should also be noted that the polymer spherulites are aggregates with diffusive interfaces rather than showing a fractal character like it was reported [25]. This confirms the recent results [5] obtained on joint spherulitic aggregates of semi-crystalline multiblock PEB-*n* copolymers and paraffin molecules in common solution. We want to underline that for the complete characterization of such complex morphologies showing a hierarchical internal organization an exploration of a wide *Q* range is required in order to avoid misinterpretation of the scattering features.

Figure 3-left presents the scattering profile at room temperature from the 0.5% solution of *a*PP-*i*PP alternating copolymer in d-26 measured over a wide *Q*-range by combining the SANS, f-SANS and ultra-SANS methods. The sample was cooled in a controlled way (1°C/min) from the single coil regime, at 180°C.

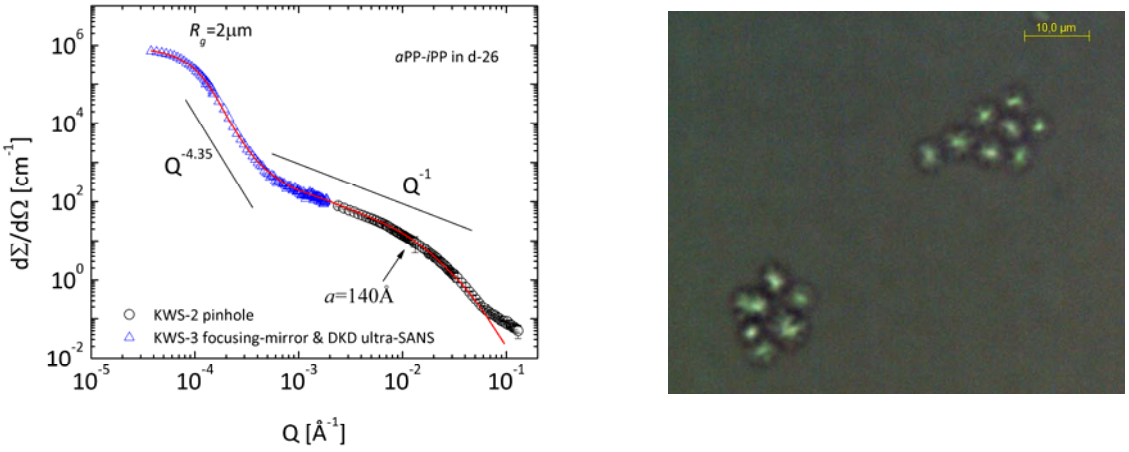

Figure 3. (left) Wide-*Q* scattering pattern from solution of *a*PP-*i*PP alternating copolymer in d-26 at room temperature; lines with the same meaning as in figure 1; (right) Morphology of *a*PP-*i*PP alternating copolymer in d-26 observed under microscope using the bright field; the scale bar represents 10µm.

The scattering pattern collected over four decades in *Q* reveals again formation of a complex morphology showing multiple structural levels and hierarchical internal organization. Large micron size aggregates with diffusive interfaces are composed of one-dimensional rod-like substructures, as revealed by the Q^{-1} behavior of the scattered intensity observed at the intermediate *Q* range. Two structural levels are revealed, the overall size of the macro-aggregates (R_g) at very low *Q* and the thickness *a* of the rods, towards high *Q*. A length of the rod *L*=0.8µm is deduced from the Beaucage fit in the crossover *Q*-region between the patterns from the macro-aggregates and the one-dimensional structures. The fact that the radius of the macro-aggregates is larger than the length of the rod-like substructures demonstrates that branching effects develop extensively in the *a*PP-*i*PP morphology. Optical micrographs (figure 3-right) show large scale aggregates displaying a spherical shape and irregular edges. With crossed polarizers no typical features of spherulitic texture were observed. This proves that the polymer aggregates are solvent-swollen dense objects showing a preponderant amorphous or diffuse behavior. The fit of the wide-*Q* scattering data using the multilevel equation of Beaucage (2) delivered the geometrical parameters (R_g of the macro-aggregates and the rod radius *a*, shown in figure 3-left) and the "forward scattering" from the two identified structures. The temperature evolution of the self-assembling of *a*PP-*i*PP alternating polymers [3] has shown that the

scattered intensity level is still increasing in decreasing the temperature down to 0°C. Therefore, at room temperature there is a partition of the dissolved polymers between the self-assembled structures and the remaining chains in solution and it is not possible to obtain independent information on the polymer volume fraction inside the aggregates and the volume fraction of rod-like and large-scale aggregates in solution from the interpretation of the "forward scattering". Nevertheless, the scattered intensity level observed at the lowest Q is very low compared to that from the *s*PP solution. This shows that the polymer volume fraction inside the alternating copolymer macro-aggregates is much lower than that inside the sPP spherulites. Finally, the tendency of the *a*PP-*i*PP alternating copolymer to form one-dimensional open structures instead of lamellar morphologies may be explained taking into account the molecular architecture in a similar way with formation of rod-like aggregates in the case of the PEB-*n* random copolymers in solution [1]: the amorphous *a*PP blocks seem to form a loose corona around the crystalline nuclei formed by the crystallizing sections of the *i*PP blocks and largely screen the cocrystallization of these nuclei, promoting thus a one-dimensional growth.

Figure 4 shows the scattering from PMMA colloids corrected with background subtraction and in the radial averaged presentation as resulted from data measured at KWS-2 with seven MgF_2 lenses and a neutron wavelength λ=17.6Å. The result obtained on the same sample at KWS-3 focusing-mirror instrument with a neutron wavelength λ=12.7Å is shown in parallel. The minimum Q value reached at KWS-2 with neutron lenses goes down to 10^{-4}Å^{-1}, which shows that more than three decades in Q range, from 0.5Å^{-1} up to 10^{-4}Å^{-1}, can be covered at a single instrument. A fit with the solid sphere form factor including the polydispersity $\sigma(R)/R$ of the particle radii reported by static light scattering (σ_0=0.06 of the log-normal size distribution), which is depicted by the solid curve in figure 4, delivered a colloidal radius of about 8100Å, a value slightly higher than that obtained by static light scattering [18]. Because of finite resolution, the minima of the form factor are smeared out in the experimental data measured at both instruments.

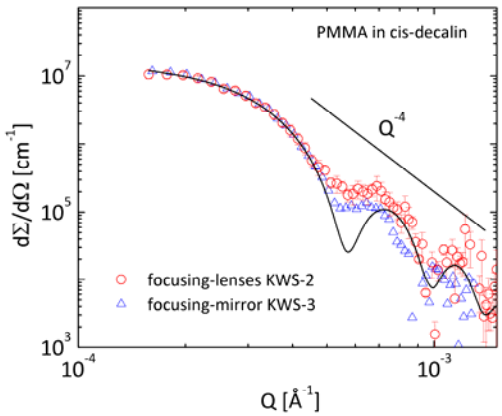

Figure 4. Intensity versus scattering vector of the 0.25% PMMA in cis-decalin solution obtained by focusing-mirror at KWS-3 and focusing-lenses at KWS-2. The solid curve represents the fit of the experimental data with the form factor of spheres (see text).

The scattering profile measured over a wide Q range from the 1% solution of the *s*PP-P(E-*co*-P) diblock copolymer in d-22 at 0°C is displayed in figure 5-left. The measurements have been performed by using the pinhole and focusing-lenses modes at KWS-2. The results obtained at KWS-3 are shown in parallel with the focusing-lenses data. The Q^{-1} power law behavior observed at low and intermediate Q-range indicates formation of long one-dimensional or rod-like aggregates. The length of these rods

is not accessible since no Guinier-like plateau is observed towards small *Q*. Thus, the length of the aggregates must exceed 1.5μm. The scattering features observed towards high *Q* relate to internal structure of the rod-like aggregates. A detailed analysis of the pinhole data as a function of temperature and polymer volume fraction in solution was done elsewhere [3]. The weak increasing tendency of the scattered intensity which is observable at very low *Q* denotes the formation of larger scale aggregates several microns in size. Figure 5-right shows the morphology of these aggregates captured at 0°C by using a thermal stage: long semi-rigid needles with a thickness of about 3μm are observed.

The straightforward attempt to model the experimental data using the cylinder form-factor [23] is hindered by the presence of a weak shoulder burying the form-factor effect of the rod's lateral size at around $Q \cong 8 \times 10^{-3}$ Å^{-1}. This feature denotes a correlation effect arising from the association of polymer rods in bundles [3]. For a detailed model analysis of the scattering data the structure factor for aligned cylinders [26] must be taken into account. A lateral size of the polymer rods of about 450Å can be roughly estimated from the deviation of the scattered intensity from Q^{-1} behavior. Combining the scattering data and the microscopy results the hierarchical character of the diblock copolymer morphology in solution is again understood: thin rods of a thickness of about 450Å, revealed by scattering, associate in bundles which, at much larger scale, appear as thick one-dimensional semi-rigid cylinders, shown by the micrographs.

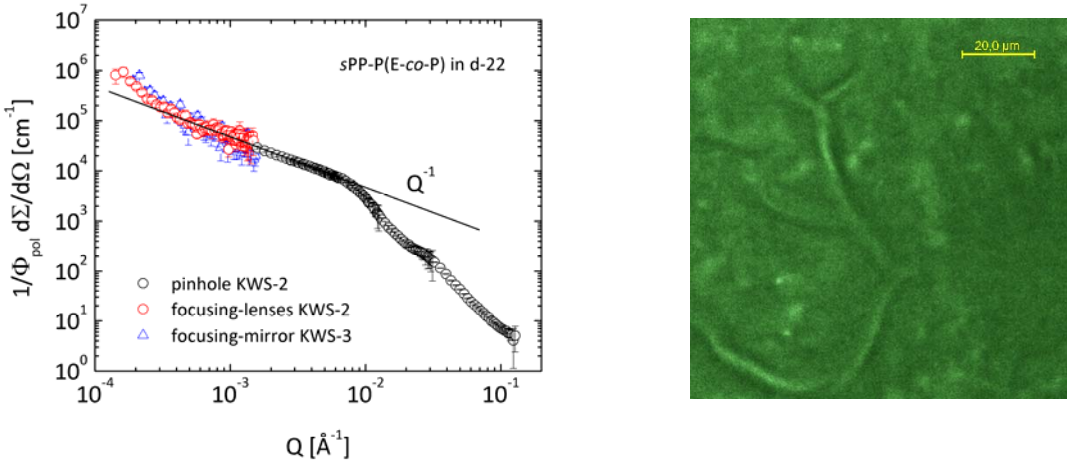

Figure 5. (left) Scattering pattern from the 1% solution of the *s*PP-P(E-*co*-P) diblock copolymer in d-22 at 0°C; (right) Morphology of *s*PP-P(E-co-P) diblock copolymer in d-22 observed under microscope; the scale bar represents 20μm.

5. Conclusion

Imaging-SANS approach combining wide-*Q* small-angle neutron scattering techniques and optical microscopy is a powerful method for the complete characterization of complex morphologies showing multiple structural levels and a hierarchical organization on a length scale between 10Å and a hundred of microns. The structural and texture features of the morphologies of interest are unambiguously elucidated, which would not be possible by using only one of the methods. A clear example is the understanding of the *s*PP spherulitic morphology which cannot be completely characterized using only microscopy observations or scattering data. Another essential message is that one needs to combine pinhole- and focusing-SANS in order to achieve a wide enough *Q*-range for avoiding misinterpretation of the scattering results. With the installation and commissioning of the MgF_2 neutron lenses at the

KWS-2 SANS diffractometer installed at the Heinz Maier-Leibnitz neutron source (FRMII reactor) in Garching, a wide *Q*-range, between 10^{-4}Å^{-1} and 0.5Å^{-1}, can be covered at a single instrument. This allows for the elimination of problems related to the sample geometry or the control of the in situ sample treatment, which are inherent when several scattering instruments are involved in the study at different time periods.

Acknowledgements
We thank Jörg Stellbrink (Forschungszentrum Jülich GmbH) for the kindness to provide us the f-SANS data on PMMA solution. Useful discussions with Dietmar Schwahn, Henrich Frielinghaus and Vitaliy Pipich (Forschungszentrum Jülich GmbH) about data interpretation are gratefully acknowledged.

References
[1] Radulescu A, Fetters L J and Richter D 2008 *Adv. Polym. Sci.* **210** 1
[2] Schaefer D W and Agamalian M M 2004 *Curr. Opin. Solid State Mater. Sci.* **8** 39
[3] Radulescu A, Mathers RT, Coates GW, Richter D and Fetters L J 2004 *Macromolecules* **37** 6962
[4] Radulescu A, Schwahn D, Stellbrink J, Kentzinger E, Heiderich M, Richter D and Fetters L J 2006 *Macromolecules* **39** 6142
[5] Radulescu A, Schwahn D, Stellbrink J, Monkenbusch M, Fetters L J and Richter S 2011 *J. Pol. Sci. Part B: Polym. Phys.* **49** 144
[6] Beaucage G, Ulibarri T A, Black E P and Schaefer D W 1995 Multiple Size Scale Structures in Silica-Siloxane Composites Studies by Small Angle Scattering *Hybrid Organic-Inorganic Composites* ed J E Mark, C I C Lee and P A Bianconi (ACS) chapter 9, pp 97-111
[7] Beaucage G, Aubert J H, Lagasse R R, Schaefer D W, Rieker T P, Erlich P, Stein R S, Kulkarni S and Whaley P D 1996 *J. Pol. Sci. Part B:Polym. Phys.* **34** 3063
[8] Schaefer D W, Rieker T, Agamalian M, Lin J S, Fischer D, Sukumaran S, Chen C, Beaucage G, Herd C and Ivie J 2000 *J. Appl. Cryst.* **33** 587
[9] Schwahn D, Meier G and Springer T 1991 *J. Appl. Cryst.* **24** 568
[10] Vad T, Sager W F C, Zhang J, Buitenhuis J and Radulescu A 2010 *J. Appl. Cryst.* **43** 686
[11] Radulescu A, Kentzinger E, Stellbrink J, Dohmen L, Alefeld B, Rücker U, Heiderich M, Schwahn D, Brückel T and Richter D 2005 *Neutron News* **16** 18
[12] Goerigk G and Varga Z 2011 *J. Appl. Cryst.* **44** 337
[13] Schwahn D and Yoo M H 1986 *Springer Proceedings in Physics* Springer Verlag: Berlin vol.2 pp 83-88
[14] Choi S M, Barker J G, Glinka C J, Cheng Y T and Gammel P L 2000 *J. Appl. Cryst.* **33** 793
[15] Koizumi S, Iwase H, Suzuki J, Oku T, Motokawa R, Sasao H, Tanaka H, Yamaguchi D, Shimizu H M and Hashimoto T 2007 *J. Appl. Cryst.* **40** s474
[16] Frielinghaus H, Pipich V, Radulescu A, Heiderich M, Hanslik R, Dahlhoff K, Iwase H, Koizumi S and Schwahn D 2009 *J. Appl. Cryst.* **42** 681
[17] Tian J, Hustad P D and Coates G W 2001 *J. Am. Chem. Soc.* **123** 5134
[18] Stellbrink J 2004 Multiple Scattering Effects in Concentrated Colloidal Solution *FRJ-2 Experimental Report, Forschungszentrum Jülich GmbH*
[19] Schaefer D W, Martin J E, Wiltzius P and Cannell D S 1984 *Phys. Rev. Lett.* **52** 2371
[20] Beaucage G 1996 *J. Appl. Cryst.* **29** 134
[21] Hammouda B 2010 *J. Appl. Cryst.* **43** 1474
[22] Ruland W 1987 *Macromolecules* **20** 87
[23] Pedersen J S 1997 *Adv. Colloid. Interface Sci.* **70** 171
[24] Granassy L, Pusztai T, Tegze G, Warren J A and Douglas J F 2005 *Phys. Rev.* E **72** 011605
[25] Owen A and Bergmann A 2004 *Polym. Int.* **53** 12
[26] Oster G and Riley D P 1952 *Acta Crystallogr.* **5** 272